Hybrid density functional study on lattice vibration, thermodynamic properties, and chemical bonding of plutonium monocarbide*

Rong Yang(杨荣)[1,2], Bin Tang(唐斌)[3], Tao Gao(高涛)[1,†], and BingYun Ao(敖冰云)[4,‡]

[1] *Institute of Atomic and Molecular Physics, Sichuan University, Chengdu* 610065, *China*
[2] *College of Materials Science and Engineering, Chongqing Jiaotong University, Chongqing* 400074, *China*
[3] *Institute of Finance & Trade, Chongqing City Management College, Chongqing* 401331, *China*
[4] *Science and Technology on Surface Physics and Chemistry Laboratory, P. O. Box* 718-35, *Mianyang* 621907, *China*

(Received 1 February 2016; revised manuscript received 4 March 2016; published online 25 May 2016)

Hybrid density functional theory is employed to systematically investigate the structural, magnetic, vibrational, thermodynamic properties of plutonium monocarbide (PuC and $PuC_{0.75}$). For comparison, the results obtained by DFT, DFT + U are also given. For PuC and $PuC_{0.75}$, Fock-0.25 hybrid functional gives the best lattice constants and predicts the correct ground states of antiferromagnetic (AFM) structure. The calculated phonon spectra suggest that PuC and $PuC_{0.75}$ are dynamically stable. Values of the Helmholtz free energy ΔF, internal energy ΔE, entropy S, and constant-volume specific heat C_v of PuC and $PuC_{0.75}$ are given. The results are in good agreement with available experimental or theoretical data. As for the chemical bonding nature, the difference charge densities, the partial densities of states and the Bader charge analysis suggest that the Pu–C bonds of PuC and $PuC_{0.75}$ have a mixture of covalent character and ionic character. The effect of carbon vacancy on the chemical bonding is also discussed in detail. We expect that our study can provide some useful reference for further experimental research on the phonon density of states, thermodynamic properties of the plutonium monocarbide.

Keywords: hybrid functional, DFT + U, plutonium monocarbide

PACS: 71.27.+a, 63.20.D–, 74.25.Bt **DOI:** 10.1088/1674-1056/25/6/067106

1. Introduction

Plutonium monocarbide has been a subject of intense interest in recent years, owing to its applications in advanced types of fast reactors. Compared with oxide fuels, it has many advantages. First, its very good thermal conductivity fits the important technological requirements for advanced reactors for higher operating temperatures. Second, plutonium monocarbide with the rock-salt structure is stable in a large domain of nonstoichiometry at high temperature, and its fusion temperature is high. Finally, high burn-up value (10% or more) can be obtained, since plutonium carbides contain a high concentration of metallic elements. These advantages can explain this interest in plutonium monocarbide. As is well known, plutonium monocarbide is a non-stoichiometric compound with the fcc Nacl-type structure.[1] PuC easily forms a defect structure with some of its carbon atom lattice sites vacated. We select $PuC_{0.75}$ as a defect structure to be investigated. In order to properly utilize carbide fuels in a reactor, their phase relationships and physical properties must be well understood. Of all the physical properties, the need for reliable thermodynamic data on carbide fuels is well recognized by both the engineer and the scientist. The vibrational properties are critical for understanding phase stability and thermal transport. So this work is concerned with the vibrational, thermodynamic properties of plutonium monocarbide (PuC and $PuC_{0.75}$). Additionally, the investigations of chemical bonding properties of PuC and $PuC_{0.75}$ from theoretical viewpoint are indispensable to their applications in the nuclear industry.

Experimental studies on the plutonium-bearing materials are challenging because of their toxic and radioactive nature. Thus, theoretical predictions appear to be especially important for plutonium monocarbide. However, the 5f-electron localization phenomena pose a considerable challenge to the theoretical research. To correctly describe the strong electron–electron interactions of f-electron systems, the traditional density functional theory (DFT), DFT plus the Hubbard U[2,3] (DFT + U), dynamical mean field theory (DMFT),[4] and hybrid density functional[5,6] have been developed. DFT + U which has been widely used depends on the Hubbard correction term. The value of $U_{\rm eff}$ must be tuned to obtain a better description of different properties. In Pu-based compounds, a value of 4 eV for $U_{\rm eff}$ was generally adopted.[7–9] Hybrid functional method does not contain any system-dependent parameters, but it needs high computational resources and times. In this work, we present results by using hybrid functionals and DFT + U.

Comparing with plutonium oxides, relatively few studies focus on plutonium carbides. Among plutonium carbides, PuC

*Project supported by the National Natural Science Foundation of China (Grant Nos. 21371160 and 21401173).
†Corresponding author. E-mail: gaotao@scu.edu.cn
‡Corresponding author. E-mail: aobingyun@caep.cn
© 2016 Chinese Physical Society and IOP Publishing Ltd

is most studied, and the studies on non-stoichiometric compound are more scarce. Experimentally, the data of structural parameters can be obtained. Experimental work[10] revealed that plutonium monocarbide undergoes a magnetic phase transition at ≈ 100 K, leading to a simple antiferromagnetic structure with Pu along the (0.0,1) direction. The observed valence-band spectra of Pu carbides were obtained by Gouder *et al.*[11] The heat content (enthalpy) of PuC above 298 K was measured with an isothermal drop calorimeter by Kruger and Savage.[12] In theory, some progress has been made in the ground-state properties of plutonium monocarbide. The structural, electronic and magnetic properties of PuC were investigated by Wen *et al.*[9] Havela *et al.*[13] studied the magnetic properties of PuC by LDA + U calculations. Petit *et al.*[14] investigate the ground-state valency configuration of Pu ions in PuC by using the self-interaction corrected local spin-density approximation. However, to our knowledge, no data of phonon spectrum are available in the literature. The accurate determination of phonon spectrum can help us to acquire thermodynamic properties such as the Helmholtz free energy ΔF, internal energy ΔE, entropy S, and constant-volume specific heat $C_{\rm v}$. In addition, the investigation of chemical bonding has not been included in the previous studies. Hence, we calculate the lattice vibrations, thermodynamic properties and chemical bonding of PuC and $PuC_{0.75}$. Our investigations, especially for nonstoichiometric compound ($PuC_{0.75}$) are of great significance.

In this work, we first investigate the crystal structures and magnetic properties of PuC and $PuC_{0.75}$, and compare the results with experimental data to check whether hybrid functional method is suitable for PuC and $PuC_{0.75}$. Then, phonon-dispersion curves of PuC and $PuC_{0.75}$ are obtained, the Raman and infrared active modes at Γ point are further assigned and presented. Next, the thermodynamic properties including ΔF, ΔE, S, and $C_{\rm v}$ are predicted for PuC and $PuC_{0.75}$. And finally, the chemical bonding properties of PuC and $PuC_{0.75}$ are discussed in detail.

The rest of this paper is organized as follows. In Section 2 we describe our computational method and details, and the results are presented and discussed in Section 3. This paper is ended with conclusions in Section 4.

2. Computational method

All our calculations are performed by using the full potential linearized augmented plane wave (FP-LAPW) method as implemented in the all electron WIEN2K code.[15,16] In the exchange–correlation functional used are GGA Perdew–Burke–Ernzerhof (PBE) formalism[17] and the local spin-density approximation (LSDA).[18] In the LSDA + U[19] calculations, the effective Hubbard U is 4.00 eV, which is used by Wen *et al.*[9] In the hybrid scheme, the PBE0 and Fock-0.25 hybrid functionals are employed. For PBE0 hybrid functional,[20,21] the exchange-correlation energy is

$$E_{\rm xc}^{\rm PBE0}[\rho] = E_{\rm xc}^{\rm PBE}[\rho] + \frac{1}{4}(E_x^{\rm HF}[\Psi_{\rm sel}] - E_x^{\rm PBE}[\rho_{\rm sel}]), \quad (1)$$

where $\Psi_{\rm sel}$ and $\rho_{\rm sel}$ refer to the wave function and the corresponding electron density of the selected electrons, respectively. For PBE0, a fraction (1/4) of HF exchange replaces the GGA (PBE) exchange but only for the selected electrons. The exchange–correlation energy of Fock-α hybrid functional[22] is

$$E_{\rm xc}^{\rm Fock-\partial}[\rho] = E_{\rm xc}^{\rm LDA}[\rho] + \partial(E_x^{\rm HF}[\Psi_{\rm sel}] - E_x^{\rm LDA}[\rho_{\rm sel}]). \quad (2)$$

The form of Eq. (2) is the same as that of Eq. (1), except LDA replacing PBE. In this work, we use $\alpha = 0.25$ for the fraction, giving functional Fock-0.25.

In our calculations of PuC, a supercell consisting of 4 Pu atoms and 4 C atoms is used. When one C atom is replaced by a vacancy, it forms C-deficient compound $PuC_{0.75}$. We should mention that the experimentation[1] confirms that the C-deficient compound has the fcc Nacl-type structure.

The muffin-tin radii have been chosen to be 2.3 a.u. and 1.6 a.u. (The unit a.u. is short for atomic unit) for Pu and C atoms, respectively. The parameter $R_{\rm MT}K_{\rm MAX} = 8.5$, where $R_{\rm MT}$ is the smallest atomic sphere radius and $K_{\rm MAX}$ is the plane wave cutoff parameter. The Brillouin zone is sampled with 100 k-points. The charge convergence is set to be 0.001 e, the total energy convergence is set to be 0.001 Ry (1 Ry = 13.6056923(12) eV), and the force convergence is set to be 0.001 Ry/a.u. In the antiferromagnetic (AFM) calculations, we take the 1k (collinear) order. The spins of Pu atoms change sign along the oz axis.

3. Results

3.1. Crystal structure and magnetic properties

We calculate the total energies for a set of different atomic volumes to determine the optimized lattice constants. The bulk modulus is obtained from fitting to Murnaghan's equation of state.[23] The band gaps, the total magnetic moment and the differences in total energy between ferromagnetic (FM) and AFM states ($\Delta E = E_{\rm FM} - E_{\rm AFM}$) are also obtained. All results are listed in Table 1.

The known experimental finding is that at room temperature the lattice parameter increases from a value of 4.953 Å to 4.973 Å as the carbon content increases from the hypo- to hyper-stoichiometric composition.[24–29] For stoichiometric PuC, the measured lattice parameter is 4.965 Å.[24] From Table 1, our calculated lattice constants of FM states are larger than those of AFM states for both PuC and $PuC_{0.75}$. The optimized lattice constants in AFM states are closer to the

experimental values, which means that the ground states of PuC and $PuC_{0.75}$ are AFM. Our calculated values of $\Delta E(= E_{FM} - E_{AFM})$ by LSDA + U and Fock-0.25 methods are positive. This also indicates that the AFM state is stabler than the FM state. The conclusion is confirmed by experimental work that an AFM transition occurs at 100 K in plutonium monocarbide.[10] However, LSDA incorrectly predicts an FM ground state of PuC.

Table 1. Complication of data on FM and AFM states of PuC and $PuC_{0.75}$: lattice constant a_0, total magnetic moment μ_{tot}, bulk modulus B_0, $\Delta E = E_{FM} - E_{AFM}$, and band gap (eV). The Hubbard parameter U is 4.0 eV.

Compound	Method	a_0/Å		μ_{tot}/μ_B		B_0/GPa		ΔE/Ry	E_{gap}/eV	
		FM	AFM	FM	AFM	FM	AFM		FM	AFM
PuC	LSDA	4.849	4.845	16.35919	0.00001	149.64	151.55	−0.0234	0.0	0.0
	LSDA + U	5.025	5.001	17.97935	0.00026	116.92	125.22	0.0139	0.0	0.0
	LSDA + U + SO	4.996	4.989	17.59776	0.00260	132.85	177.62	0.0022	0.0	0.0
	Fock-0.25	4.989	4.961	15.52696	−0.00007	209.98	177.40	0.0469	0.0	0.0
	Fock-0.25 + SO	4.947	4.935	15.50289	0.00001	219.44	180.60	0.0037	0.0	0.0
	PBE0	5.062	5.057	17.42156	0.00001	113.91	148.64	0.0339	0.0	0.0
	Exp[a)]	4.965		–		–		–	–	
	HSE[b)]	5.043	5.115	17.40000	–	–		–	0.0	0.0
	SIC-LSD[c)]	–	4.910	–		–	172.00	–	–	
$PuC_{0.75}$	LSDA	4.833	4.810	17.41930	–0.09581	121.22	129.17	0.0052	0.0	0.0
	LSDA + U	5.040	5.032	19.21957	–1.12160	155.96	112.92	0.0538	0.0	0.0
	LSDA + U + SO	5.009	5.031	19.24940	–0.40972	146.16	107.14	0.0009	0.0	0.0
	Fock-0.25	4.900	4.956	15.19138	–0.65620	164.71	150.84	0.0220	0.0	0.0
	Fock-0.25 + SO	4.898	4.896	14.24475	–0.32182	124.90	137.48	0.0043	0.0	0.0
	PBE0	5.017	5.030	14.24475	–0.32182	85.30	92.38	0.0043	0.0	0.0

[a)] Ref. [24], [b)] Ref. [9], [c)] Ref. [14].

Of all the methods, Fock-0.25 yields the very accurate lattice constants. For example, for PuC in the AFM state, the value 4.961 Å deviates from the experimental data only by 0.004 Å. But PBE0 severely overestimates the lattice parameter in FM (or AFM) state. This indicates that GGA (PBE) is not suitable for plutonium monocarbide. When a C atom is removed from PuC to form C-deficient compound $PuC_{0.75}$, a decrease of lattice constant is found in Table 1. For example, the lattice parameter of $PuC_{0.75}$ is reduced by about 0.005 Å from Fock-0.25 in the AFM state. It means that the additional removal of a C atom makes lattice contraction. The measured lattice constant increases from 4.953 Å to 4.973 Å as the carbon content increases. So our results are in good agreement with the experimental results.

As expected, the lattice parameter increases as long as the electron correlation (U or hybrid functional) is included. When Hubbard U increases from 0 to 4 eV, the localization of the 5f electrons of Pu will be enhanced, while the cohesion of the crystal is further reduced, which leads to the increase of the lattice constant. Moreover, we consider the effects of spin-orbit coupling (SO). When SO is included, the lattice parameter is reduced slightly in LSDA + U + SO/Fock-0.25 + SO framework compared with that in the LSDA + U/Fock-0.25, which is similar to the Pu–H systems calculated by Guo *et al.*[8] From the energy differences between the FM and AFM states in LSDA + U + SO/Fock-0.25 + SO framework, the ground states of PuC and $PuC_{0.75}$ are also AFM. So spin–orbit coupling has little effect on crystal structure and magnetic properties of PuC and $PuC_{0.75}$. Furthermore, the lattice constants of PuC and $PuC_{0.75}$ in Fock-0.25 are much closer to the experimental values than those obtained by LSDA + U + SO/Fock-0.25 + SO. Thus, SO is not taken into account in the following calculations.

From our calculated band gaps, both PuC and $PuC_{0.75}$ are conductors. It is true since plutonium monocarbide is metal. Finally, we compare our results with other theoretical values (HSE[9] and SIC-LSD[14]). We find that our calculated lattice parameters obtained by Fock-0.25 are much better than the others, suggesting that the advantage of the present method (Fock-0.25) over the others for plutonium monocarbide. For the bulk modulus B_0, our calculated value 177.40 GPa from Fock-0.25 can be compared with the result 172.00 GPa from SIC-LSD.[14]

On the whole, Fock-0.25 gives the best structural properties and predicts AFM phase, which supplies the safeguard for the following calculations of vibrational and thermodynamic properties of PuC and $PuC_{0.75}$. For comparison, LSDA + U calculations will be also performed in the following studies. While PBE0 is not adopted in the following calculations, since the optimized lattice parameters are not reproduced well by PBE0.

3.2. Vibrational properties

Our phonon calculations are performed by the small displacement method.[30] Since the space groups of PuC and $PuC_{0.75}$ are Fm-3m (225), PuC and $PuC_{0.75}$ belong to O_h point

group. The high-symmetry points selected in the calculations are Γ(0, 0, 0), X (0.5, 0, 0.5), W (0.5, 0.25, 0.75), and L (0.5, 0.5, 0.5). For stoichiometric PuC, there are two atoms in a primitive cell. Thus, this system contains three acoustic modes and three optical modes, that is, two optical transverse branches and one optical longitudinal branch, two acoustic transverse branches and one acoustic longitudinal branch are included. The phonon dispersion curves of PuC obtained from Fock-0.25 and LSDA + U are shown in Figs. 1(a) and 1(b), respectively. From Fig. 1, we find no imaginary frequencies, which indicates that PuC is dynamically stable at ambient pressure and 0 K. It is obvious that the phonon dispersion curves obtained by Fock-0.25 and LSDA + U methods do not differ greatly. The biggest difference is the value of the gap between the acoustic and optical branch. For LSDA + U, the gap is 2.78 THz, and the gap is 4.43 THz for Fock-0.25. The difference can be explained as follows. In the LSDA + U ($U_{\rm eff} = 4.0$ eV) method, the localization of Pu 5f electron is more strengthened, the corresponding contribution to Pu–C covalent bonding is more weakened, while the ionic character is more enhanced, which results in the decrease of lattice vibration energy. On the basis of point group theory, the irreducible representations of the acoustic mode and optical mode in the center of the BZ are: $\Gamma_{\rm acoustic} = T_{1u}$, and $\Gamma_{\rm optical} = T_{1u}$, respectively. Here T_{1u} is infrared-active. The phonon frequencies for infrared-active modes T_{1u} obtained with Fock-0.25 and LSDA + U at Γ point are 297.66 cm^{-1} and 228.29 cm^{-1}, respectively. These data need to be checked by future experiments. Considering the fact that Fock-0.25 gives the best structural properties, Fock-0.25 framework can describe the dynamical properties of PuC reasonably. The phonon partial densities of states (PPDOSs) of PuC from Fock-0.25 and LSDA + U are plotted in Fig. 2. Since Pu atom is heavier than C atom, the vibration frequency of Pu is lower than that of C atom.

Now we discuss the lattice dynamical properties of $PuC_{0.75}$. For simplicity, we only show the results from Fock-0.25. From Fig. 3(a), the calculated phonon dispersion curves have no soft modes, which indicates that PuC is dynamically stable. Since the primitive cell contains 7 atoms, there are 3 acoustic modes and 18 optical ones. According to the group-theoretical analysis, the irreducible representations at the BZ are $\Gamma_{\rm acoustic} = T_{1u}$ and $\Gamma_{\rm optical} = 4T_{1u} + 2T_{2u}$. Here T_{1u} is infrared-active and T_{2u} is silent mode. The calculated phonon frequencies at Γ point are listed in Table 2. Figure 3(b) shows the PPDOSs of $PuC_{0.75}$. It is very easy to observe that along the frequency axis, there are two frequency gaps whose widths are 5.13 THz and 1.33 THz. And we note that the PPDOSs of each Pu atom distinguish each other and the PPDOSs of each C atom are almost the same as those of $PuC_{0.75}$. The reason is that the crystal symmetry is destroyed when a C atom is removed from PuC.

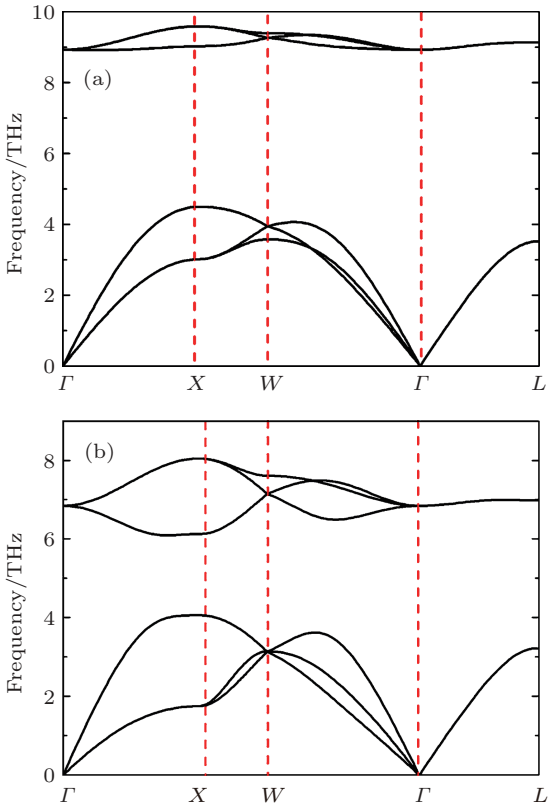


Fig. 1. (color online) Calculated phonon dispersion curves from (a) Fock-0.25 and (b) LSDA + U for PuC.

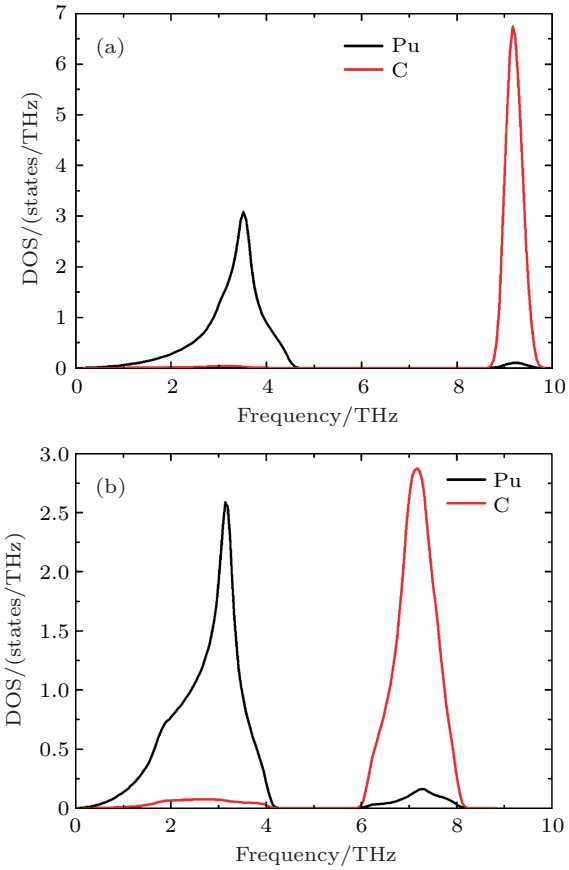


Fig. 2. (color online) Calculated phonon partial densities of states (PPDOSs) from (a) Fock-0.25 and (b) LSDA + U for PuC.

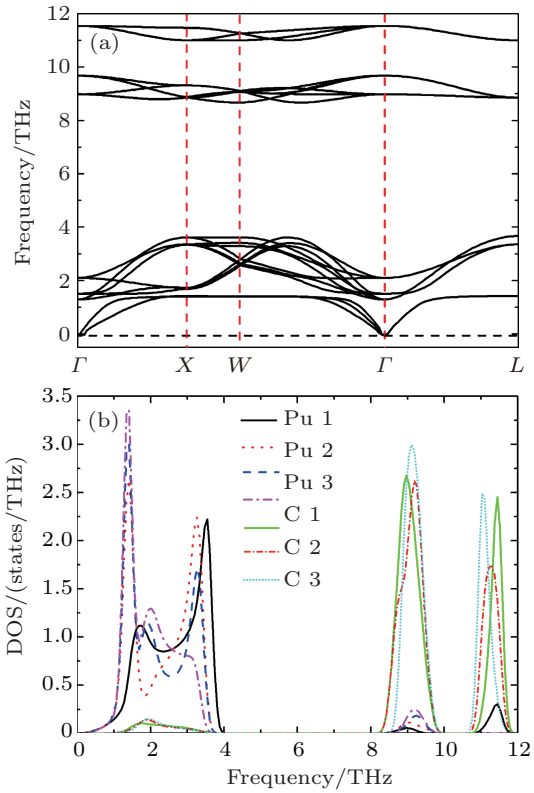


Fig. 3. (color online) Calculated (a) phonon dispersion curves and (b) partial density of phonon states (PPDOSs) from Fock-0.25 for $PuC_{0.75}$.

Table 2. Calculated phonon frequencies (in cm^{-1}) and the assignment of the infrared-active and silent modes at Γ point of $PuC_{0.75}$.

IR	Silent
T_{1u}	T_{2u}
43.12	69.97
50.35	322.82
299.50	
384.96	

To our knowledge, there are currently no experimental or theoretical data for the vibrational properties of PuC and $PuC_{0.75}$. We hope our results can provide useful reference for the further research on the vibrational properties of PuC and $PuC_{0.75}$.

3.3. Thermodynamic properties

Thermodynamic properties of solid materials can be determined by the calculated phonon density of states in the quasiharmonic approximation (QHA). The expressions of the Helmholtz free energy ΔF, internal energy ΔE, entropy S, and constant-volume specific heat C_v are given, respectively, by[31]

$$\Delta E = 3nN\frac{\hbar}{2}\int_0^{w_L} w\coth\left(\frac{\hbar w}{2k_BT}\right)g(w)\,\mathrm{d}(w), \quad (3)$$

$$\Delta F = 3nNk_BT\int_0^{w_L}\ln\left\{2\sinh\left(\frac{\hbar w}{2k_BT}\right)\right\}g(w)\,\mathrm{d}(w), \quad (4)$$

$$S = 3nNk_B\int_0^{w_L}\left[\frac{\hbar w}{2k_BT}\coth\frac{\hbar w}{2k_BT} - \ln\left\{2\sinh\left(\frac{\hbar w}{2k_BT}\right)\right\}\right]g(w)\,\mathrm{d}(w), \quad (5)$$

$$C_v = 3nNk_B\int_0^{w_L}\left(\frac{\hbar w}{2k_BT}\right)^2\mathrm{csch}^2\left(\frac{\hbar w}{2k_BT}\right)g(w)\,\mathrm{d}(w), \quad (6)$$

where w is the phonon frequency, $g(w)$ is the normalized phonon DOS, N is the number of unit cells, k_B and $\hbar$ refer to the Boltzman constant and reduced Planck constant, respectively. At zero temperature, the ΔF and ΔE can be expressed as $\Delta F_0 = \Delta E_0 = 3nN\int_0^{w_L}(\hbar w/2)g(w)\,\mathrm{d}w$. Figure 4 shows the computed ΔE, ΔF, S, and C_v of PuC each as a function of temperature in the Fock-0.25 framework. We can find that $\Delta E_0 = \Delta F_0 = 7.4$ K·J/mol and ΔE increases almost linearly with temperature rising. From Fig. 4(b), the vibrational entropy curve increases smoothly with the increase of temperature due to the vibrational frequency increasing with temperature. At high temperature (over 800 K), our calculated C_v tends to be a constant of 49.6 J/(K/mol), which almost approaches to the Dulong–Petit limit. The Dulong–Petit law[32] is $C_v = 3N*R$, where N is the number of atoms and R is the gas constant. For PuC, there are two atoms in one formula, which means that the theoretical value should be 49.9 J/(K/mol). Obviously, the deviation between our value and theoretical value is only 0.6%.

The observed changes in enthalpy of PuC with temperature rising are listed in Table 3, along with our calculated ones. Here, the change in enthalpy is acquired by the equation $\Delta H = \Delta E + P\Delta V$, where E refers to the internal energy, P the pressure, and V the volume.[33] In solid and liquid phases, the change in term $P\Delta V$ is very small compared with in term ΔE. And we set the equilibrium pressure to be zero. So, $\Delta H \approx \Delta E$. Comparing the data in Table 3, our calculated ΔH from Fock-0.25 and LSDA + U are in good agreement with the experimental results. The slightly larger deviation of ΔH under high temperature may be due to the limitation of the QHA. In our calculations, all the vibrational eigenvalues are obtained at $T = 0$ K. With the increase of temperature, the volume dependence of phonon free energy changes, then the equilibrium volume changes with temperature. The high-order anharmonicity at high temperature may become more prominent than at low temperature for Pu monocarbide.

Table 3. Calculated values of H–H_{298} (K·J/mol) and the corresponding experimental data of PuC.

	425.2 K	427.6 K	525.2 K	530.1 K	628.0 K	733.2 K	825.2 K	830.5 K	921.7 K
Fock-0.25	6.005	6.113	10.800	11.031	15.790	20.945	25.455	25.691	30.240
LSDA + U	6.079	6.184	10.944	11.177	15.971	21.178	25.715	25.992	30.522
Expt.[a)]	5.990	5.745	11.054	11.006	16.460	22.108	28.049	27.416	32.626

[a)] Ref. [12].

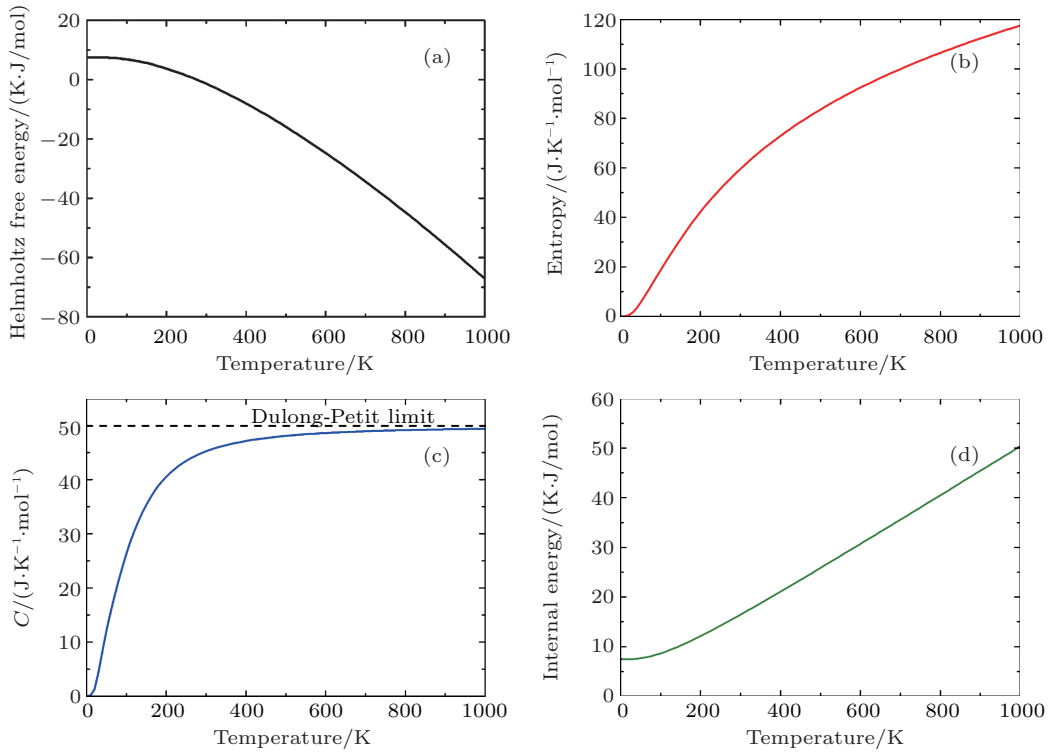


Fig. 4. (color online) Calculated (a) the Helmholtz free energy ΔF, (b) the entropy S, (c) the constant-volume specific heat $C_{\rm v}$, and (d) the internal energy ΔE of PuC in the Fock-0.25 framework.

Listed in Table 4 are our calculated $S_{\rm T}$–S_{298} (J/(K/mol)) and heat capacity (J/(K/mol)) of PuC using QHA, comparison with previous theoretical data.[12] These quantities are calculated for a temperature of 1900 K, which is 50 K below the melting point of PuC.[34] $C_{\rm p}$ and $C_{\rm v}$ are related by the following equation[35]

$$C_{\rm p} = C_v + T\left(\frac{\partial V}{\partial T}\right)_{\rm p}\left(\frac{\partial P}{\partial T}\right)_V\Big|_{V=V_0(T)} = C_v + \partial^2 BVT, \quad (7)$$

where α is the volume thermal expansion coefficient, B is the bulk modulus, V is the volume, and T is absolute temperature. Kruger and Savage[12] calculated $C_{\rm p}$ according to the equation $C_{\rm p} = 13.08 + 11.44 \times 10^{-4}T - 3.232 \times 10^5 T^{-2}$ suggested by Maier and Kelley.[36] From Table 4, the entropy difference $S_{\rm T}$–S_{298} obtained by us can also be compared with other theoretical results. Besides the limitation of the QHA, we only consider the vibration entropy and ignore the electronic contribution to the entropy in our calculations, which leads to the increase of difference between our data and the values of Kruger and Savage as temperature rises. Certainly, the $C_{\rm v}$ values are different from the $C_{\rm p}$ values at high temperatures according to Eq. (7).

Table 4. Our calculated values of $S_{\rm T}$–S_{298} (J/(K/mol)) and heat capacity (J/(K/mol)) of PuC, along with other theoretical values.

T/K	$(S_{\rm T} - S_{298})$/(J/(K/mol))			Heat capacity (J/(K/mol))		
	Fock-0.25	LSDA + U	Other[a)]	$C_{\rm v}$ (Fock-0.25)	$C_{\rm v}$ (LSDA + U)	$C_{\rm p}$ (other)[a)]
400	13.292	13.669	13.209	47.171	48.175	48.154
500	23.951	24.495	24.369	48.115	48.778	51.665
600	32.771	33.398	24.369	48.643	49.112	53.797
700	40.295	41.006	42.427	48.967	49.315	55.260
800	46.816	47.610	49.909	49.180	49.448	56.388
900	52.626	53.420	56.514	49.327	49.540	57.308
1000	57.851	58.645	62.742	49.432	49.605	58.102
1100	62.533	63.369	68.301	49.510	49.654	58.813
1200	66.838	67.716	73.443	49.570	49.691	59.481
1300	70.809	71.687	78.082	49.617	49.720	60.108
1400	74.488	75.324	82.639	49.654	49.743	60.652
1500	77.915	78.793	86.819	49.684	49.761	61.279
1600	81.121	82.005	90.898	49.708	49.776	61.854
1700	84.135	85.023	94.623	49.728	49.789	62.440
1800	86.978	87.869	98.222	49.745	49.799	62.942
1900	89.668	90.562	101.700	49.760	49.808	63.445

[a)] Ref. [12].

For $PuC_{0.75}$, we also investigate its thermodynamic properties. In Table 5 listed are our calculated values of S, H–H_{298}, and C_v at selected temperatures. Several authors have measured the absolute entropies of nonstoichiometric plutonium carbides at 298.15 K. Their results are 18.2,[37] 21.2,[38] 15.3,[39] and 17.2[40] cal/(mol/K). The value estimated by us is 15.3 cal/(mol/K) in Fock-0.25 scheme. So our calculated value agrees reasonably with the experimental data. The curves of ΔE, ΔF, S, and C_v versus temperature are shown in Fig. 5. The C_v of $PuC_{0.75}$ also follows the Debye model, and is also close to the classic limit (43.6 J/(K/mol)) which is called Dulong–Petit's law[32] at high temperatures (over 800 K).

Table 5. Our calculated values of H–H_{298} (K·J/mol), S (J/(K/mol)), and C_v (J/(K/mol)) of $PuC_{0.75}$.

	298 K	400 K	500 K	600 K	700 K	800 K	900 K	1000 K
H–H_{298}	0	4.077	8.264	12.507	16.784	21.083	25.397	29.720
S	64.186	75.906	85.244	92.979	99.572	105.312	110.393	114.948
C_v	39.913	41.441	42.202	42.632	42.896	43.070	43.190	43.276

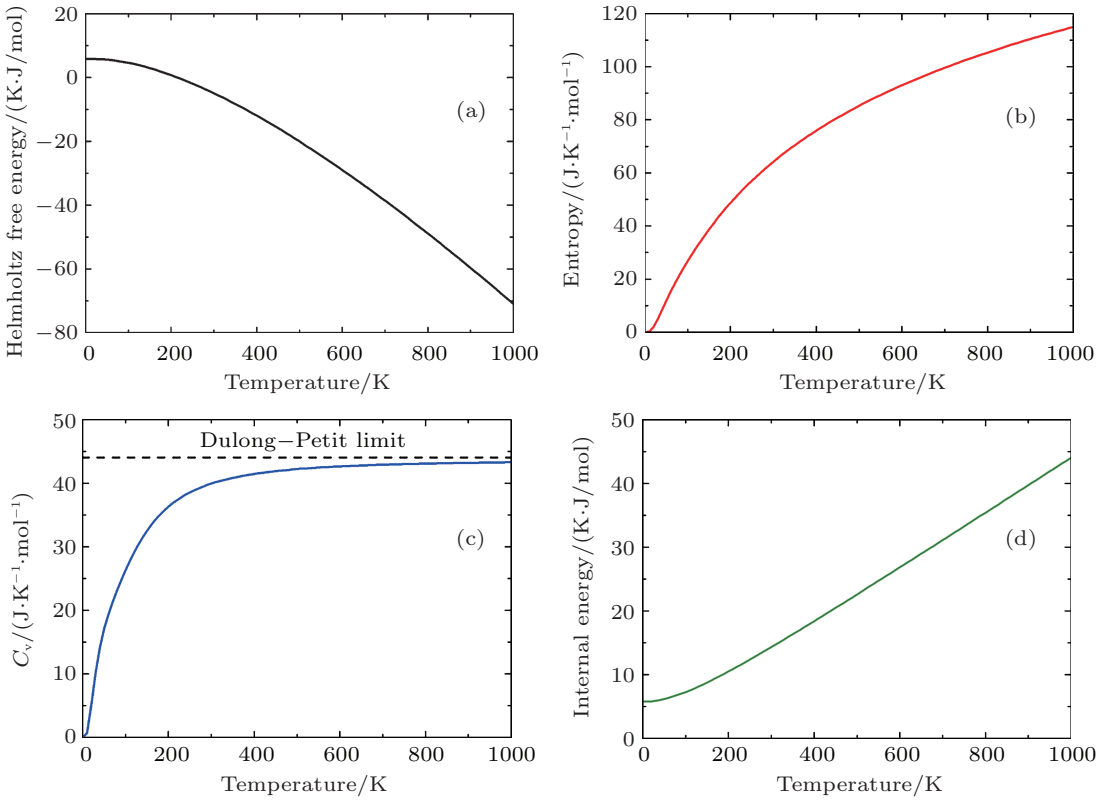


Fig. 5. (color online) Calculated (a) the Helmholtz free energy ΔF, (b) the entropy S, (c) the constant-volume specific heat C_v, and (d) the internal energy ΔE of $PuC_{0.75}$ in the Fock-0.25 framework.

3.4. Chemical bonding

In this section, we will analyze the Pu–C bonds of PuC and $PuC_{0.75}$. The charge densities and the difference charge densities along the (001) plane of PuC and $PuC_{0.75}$ are shown in Figs. 6 and 7, respectively. The difference charge density is obtained from the equation[41]

$$\delta\rho = \rho(\mathrm{PuC}/\mathrm{PuC}_{0.75}) - \rho(\mathrm{Pu}) - \rho(\mathrm{C}), \tag{8}$$

where ρ is the valence-electron charge density. Figures 6(a) and 7(a) both show that the highest density charge piles up in the immediate vicinity of the nuclei, while the charge densities are relatively low in the interstitial regions. It reflects that most of the electrons are firmly bound up around atomic nuclei, and only a few valence electrons can escape from their bondage. For the nearest Pu–C atoms, the charge density distribution is largely deformed toward their bonds, which implies significant covalent character in the bonding of Pu and C atoms. This is associated with the hybridization between Pu-6d and C-2p states, which can be seen from the partial densities of states (Fig. 8). In Figs. 6(b) and 7(b), the orange zone and blue zone represent the gain of charge and the loss of charge respectively. It is clear that a great quantity of charges of Pu atoms move to C atoms for PuC and $PuC_{0.75}$. So, the bonding between Pu and C atoms also has an ionic character. Compared PuC with $PuC_{0.75}$, Pu ions in $PuC_{0.75}$ are ionized somewhat less than Pu ions in PuC. This can be explained in the following. That one C atom is replaced by a vacancy means the breaking of some

Pu–C bonds, which leads to the growing of plutonium states in this region and their delocalization toward Pu–Pu bonds near the lattice defect.

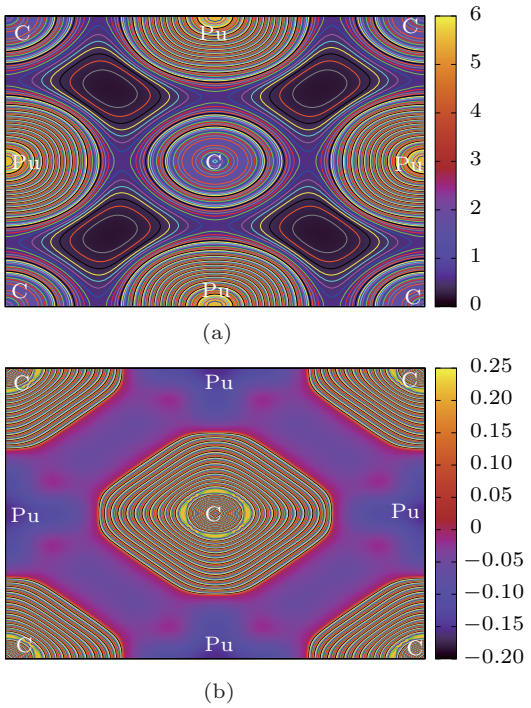


Fig. 6. (color online) Contour plots of (a) charge density and (b) charge density difference along the (001) plane in Fock-0.25 calculations for PuC.

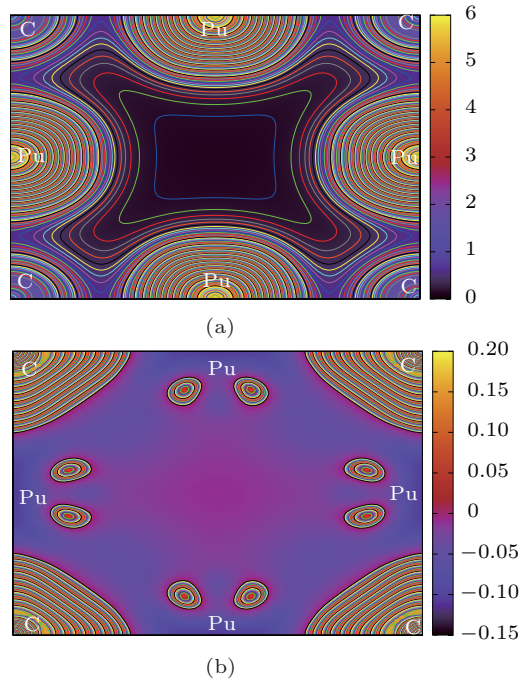


Fig. 7. (color online) Contour plots of (a) charge density and (b) charge density difference along the (001) plane in Fock-0.25 calculations for $PuC_{0.75}$.

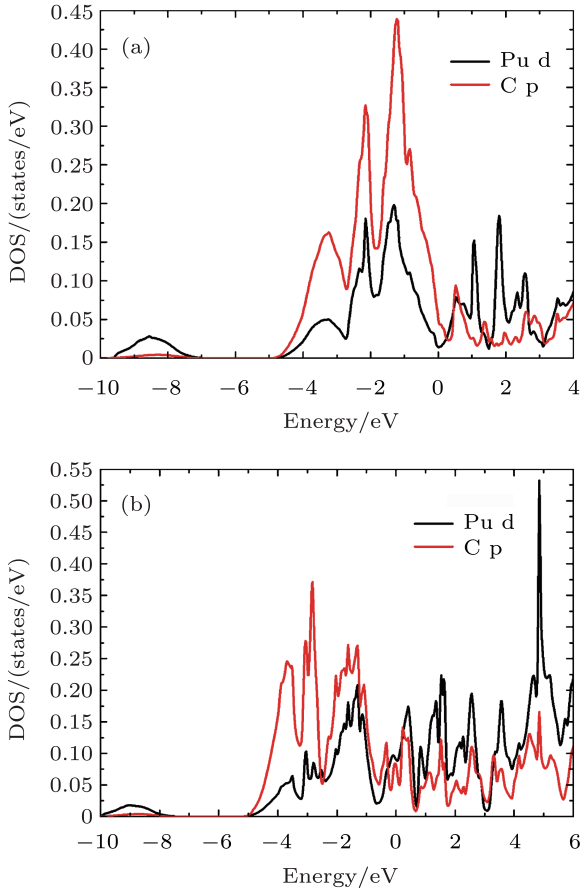


Fig. 8. (color online) Partial densities of states for the Pu d and C p of (a) PuC (b) $PuC_{0.75}$ in Fock-0.25 calculations.

The charge transfer between the Pu atom and the C atom is quantified by the Bader charge analysis.[42] As is well known, Pu atom has 16 electrons outside the core, and C atom has 4 electrons outside the core. All results are listed in Table 6. When one C atom is replaced by a vacancy, the crystal symmetry is destroyed. So for $PuC_{0.75}$, Pu atoms are divided into two categories: one is near the vacancy which is marked as Pu_2, the other is far from the vacancy which is denoted as Pu_1. From Table 6, each Pu atom losses $1.14|e|$ and the charge of $1.14|e|$ is transferred to C atom in PuC system. The result suggests that any directional bonding of the C atom to Pu atom is ionic and small. While for $PuC_{0.75}$, one Pu atom far from the vacancy (Pu_1) still losses $1.14|e|$, each Pu atom near the vacancy (Pu_2) losses $0.83|e|$, and these charges are transferred to three C atoms. Thus, the ionic character of the $PuC_{0.75}$ system is weaker than that of the PuC system near the vacancy, which is similar to the result of the difference charge densities (Fig. 6(b) and Fig. 7(b)) as mentioned above.

Table 6. Calculated bader charges (Q_B) and bader volumes (V_B) for AFM PuC and AFM $PuC_{0.75}$ in Fock-0.25 framework.

Compound	$Q_B(Pu_1)/e$	$Q_B(Pu_2)/e$	$Q_B(C)/e$	$V_B(Pu_1)/Å^3$	$V_B(Pu_2)/Å^3$	$V_B(C)/Å^3$
PuC	14.86	–	5.14	16.66	–	9.32
$PuC_{0.75}$	14.86	15.17	5.21	15.95	18.68	9.21

According to the charge densities and the difference charge densities, the partial densities of states, the Bader charge analyses for PuC and $PuC_{0.75}$, we can reach the following conclusion. (i) Mixtures of covalent and ionic character are present in the Pu–C bonds of PuC and $PuC_{0.75}$. (ii) The ionic character is stronger than the covalent character in the PuC system. (iii) Near the vacancy, Pu ions in $PuC_{0.75}$ are ionized somewhat less than Pu ions in PuC, and the ionic character is weaker than the covalent character in the $PuC_{0.75}$ system. (iv) Pu–Pu bonds near the vacancy are strengthened.

The observed valence-band spectra[11] of PuC_{1-x} are characterized by the fingerprint of a triplet of sharp features, located at (or slightly below) the Fermi energy, 0.50 eV and 0.85 eV. And the spectra are dominated by the 5f character. So at the end of this section, we give the total and partial densities of states for $PuC_{0.75}$ in Fock-0.25 scheme for comparison. From Fig. 9, our calculated spectrum ranging from 0 eV to 3 eV almost originates from Pu atoms, and the DOS of Pu atoms is almost dominated by the 5f partial DOS. Furthermore, our spectra also have three sharp peaks which are located at −0.04, 0.34, and 0.88 eV (see Fig. 9). Thus, our results relatively well describes the observed feature of three sharp peaks.

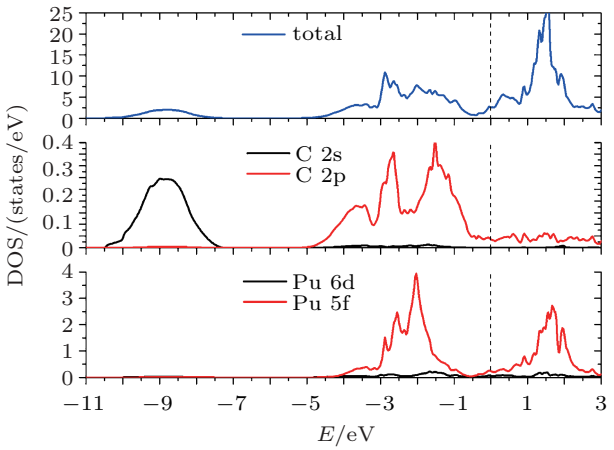


Fig. 9. (color online) Total and partial densities of states for $PuC_{0.75}$ in Fock-0.25 calculations.

4. Conclusions

The lattice vibrations, thermodynamic properties and chemical bondings of PuC and $PuC_{0.75}$ are systematically studied by using first-principle calculations. Since PuC and $PuC_{0.75}$ are strongly correlated materials, DFT + U and hybrid density functional which replaces part of the DFT exchange by 25% exact HF exchanges are employed. The optimized lattice constants are in good agreement with known experimental data. LSDA + U and Fock-0.25 successfully predict the correct ground states of AFM PuC and $PuC_{0.75}$ reported in experiments. We adopt the LSDA + U and Fock-0.25 to study the phonon dispersion curves and the corresponding PPDOSs of PuC and $PuC_{0.75}$. The infrared active and silent modes at Γ point are further assigned. On the basis of the phonon DOS, we also systematically predict the thermodynamic properties of PuC and $PuC_{0.75}$. The calculated values of H–H_{298}, S_T–S_{298}, and S are in reasonably agreement with the experimental or theoretical values. The present results indicate that our computational methods are feasible and our prediction of the dynamical properties is believable. Through the charge densities, the difference charge densities, the partial densities of states, and the Bader charge analyses, we also carry out systematical studies of chemical bonding. We find that the mixtures of covalent and ionic character are present in the Pu–C bonds of PuC and $PuC_{0.75}$. That one C atom is replaced by a vacancy leads to the growing of plutonium states in this region and their delocalization toward Pu-Pu bonds near the lattice defect. We expect that our work can provide some valuable information about the plutonium monocarbide for further experimental investigations.

Acknowledgment

The authors are grateful to the Center of High Performance Computing Physics discipline of Sichuan University for computing.

References

[1] Zachariasen W H 1949 *The Crystal Structure of Plutonium Nitride and Plutonium Carbide, The Transuranium Elements, National Nuclear Energy Series. IV*–14*B* (New York: McGraw-Hill Book Co., Inc.) p. 1448
[2] Anisimov V I, Solovyev I V, Korotin M A, Czyzyk M T and Sawatzky G A 1993 *Phys. Rev. B* **48** 16929
[3] Solovyev I V, Dederichs P H and Anisimov V I 1994 *Phys. Rev. B* **50** 16861
[4] Shim J H, Haule K and Kotliar G 2007 *Nature* **446** 513
[5] Becke A D 1993 *J. Chem. Phys.* **98** 1372
[6] Becke A D 1993 *J. Chem. Phys.* **98** 5648
[7] Wang B T and Zhang P 2011 *Chin. Phys. Lett.* **28** 047101
[8] Guo Y, Ai J J, Gao T and Ao B Y 2013 *Chin. Phys. B* **22** 057103
[9] Wen X D, Martin R L, Scueria G E, Rudin S P and Batista E R 2013 *J. Phys. Chem. C* **117** 13122
[10] Green J L, Arnold G P, Leary J A and Nereson N G 1967 *J. Nucl. Mater.* **23** 231
[11] Gouder T, Havela L, Shick A B, Huber F, Wastin F and Rebizant J 2007 *J. Phys.: Condens. Matter* **19** 476201
[12] Kruger O L and Savage H 1964 *J. Chem. Phys.* **40** 3324
[13] Havela L, Shick A and Gouder T 2009 *J. Appl. Phys.* **105** 07E130
[14] Petit L, Savane A, Szotek Z, Temmerman W M and Stoks G M 2009 *Phys. Rev. B* **80** 045124
[15] Blaha P, Schwarz K, Madsen G K H, Kvasnicka D and Luitz J 2011 *WIEN2k — an Augmented Plane Wave + Local Orbitals Program for Calculating Crystal Properties* (Austria: Karlheinz Schwarz Technische Universität Wien)
[16] Singh D J 1994 *Planewaves, Pseudopotentials and the LAPW Method* (Boston: Kluwer Academic)
[17] Perdew J P, Burke K and Ernzerhof M 1996 *Phys. Rev. Lett.* **77** 3865
[18] Vosko S H, Wilk L and Nusair M 1980 *Can. J. Phys.* **58** 1200
[19] Liechtenstein A I, Anisimov V I and Zaanen J 1995 *Phys. Rev. B* **52** 5467
[20] Ernzerhof M and Scuseria G E 1999 *J. Chem. Phys.* **110** 5029
[21] Adamo C and Barone V 1999 *J. Chem. Phys.* **110** 6158
[22] Moreira I de P R, Illas F and Martin R L 2002 *Phys. Rev. B* **65** 155102
[23] Murnaghan F D 1944 *Proc. Natl. Acad. Sci. USA* **30** 244
[24] Benedict U, Dufour C and Scholten O 1978 *J. Nucl. Mater.* **73** 208

[25] Mulford R N R, Ellinger F H, Hendrix G S and Albrecht E D 1961 *The Plutonium–Carbon System, Plutonium* 1960 (London: Cleaver-Hume Press Ltd.) p. 301
[26] Rosen S, Nevitt M V and Mitchell A W 1963 *J. Nucl. Mater.* **10** 90
[27] Kruger O L 1963 *J. Am. Ceram. Soc.* **46** 80
[28] Pascard R 1961 *E'tudes preliminaires sur le systeme plutonium-carbone et les solutions solides carbure d'uranium-carbure de plutonium, in Powder Metallurgy In the Nuclear Age. Plansee Proceedings* (Metallwerk Plansee AC, Reutte/Tyrol (1C62)) p. 387
[29] Burnham J B, Skavdahl R E and Chikalla T D 1964 *Plutonium Bearing Refractory Carbides, Carbides in Nuclear Energy*, Vol. 1. (London: Macmillan and Co. Ltd.) p. 51
[30] Alfè D 2009 *Comput. Phys. Commun.* **180** 2622
[31] Lee C and Gonze X 1995 *Phys. Rev. B* **51** 8610
[32] Petit A T and Dulong P L 1819 *Annales. de. chimie. et. de. physique.* (in French) **10** 395
[33] Limpijumnong S and Jungthawan S 2004 *Phys. Rev. B* **70** 054104
[34] Mulford R N R, Ellinger F H, Hendrix G S and Albrecht E D 1961 *in Plutonium* 1960 (London: Cleaver-Hume Press Ltd.) p. 301
[35] Wang R, Wang S F, Wu X Z and Song T T 2012 *Int. J. Thermophys.* **33** 300
[36] Maier C G and Kelley K K 1932 *J. Am. Chern. Soc.* **54** 3243
[37] Rand M H and Street R S 1964 *Anomalous Thermal Expansions in the Plutonium Monocarbide Region, Carbides in Nuclear Energy*, Vol. 1. (London: Macmillan and Co. Ltd.) p. 108
[38] Rand M H and Street R S 1962 *High Temperature X-ray Diffraction Studies,* Part 3*, Plutonium Nitride and Plutonium Sesquicarbide* (AERE-M-73)
[39] Leary J A, Thomas R L, Ogard A E and Worm G C 1964 *Thermal Conductivity and Electrical Resistivity of* UC*, (*U, Pu)C*, and* PuC*. Carbides in Nuclear Energy*, Vol. 1. (London: Macmillan and Co. Ltd.) p. 365
[40] Moser J B and Kruger O L *Thermal Diffusivity of Aetinide Compounds, Thermal Conductivity, Proceedings of Seventh Conference*, p. 302
[41] Hector L G, Herbst J F and Capehart T W 2003 *J. Alloys Compd.* **353** 74
[42] Bader R F W 1990 *Atoms in molecules: a uantum theory* (New York: Oxford University Press)